Nod2 regulates the host response towards microflora by modulating T cell function and epithelial permeability in mouse Peyer's patches

Frédérick Barreau, Chrystèle Madre, Ulrich Meinzer, et al.

Gut 2010 59: 207-217 originally published online October 15, 2009
doi: 10.1136/gut.2008.171546

Nod2 regulates the host response towards microflora by modulating T cell function and epithelial permeability in mouse Peyer's patches

Frédérick Barreau,[1,2] Chrystèle Madre,[1,2] Ulrich Meinzer,[1,2] Dominique Berrebi,[2,3] Monique Dussaillant,[1,2] Françoise Merlin,[1,2] Lars Eckmann,[4] Mickael Karin,[5] Ghislaine Sterkers,[6] Stéphane Bonacorsi,[7,8] Thécla Lesuffleur,[1,2] Jean-Pierre Hugot[1,2,9]

► See Editorial, p 153

► Supplementary figures and tables are published online only at http://gut.bmj.com/content/vol59/issue2

[1]INSERM, U843, Paris, France [2]UMR843, Université Paris Diderot, Paris, France [3]Service d'anatomie pathologique, Hôpital Robert Debré, AP-HP, Paris, France [4]Department of Medicine, School of Medicine, University of California San Diego, La Jolla, California, USA [5]Laboratory of Gene Expression and Signal Transduction, Department of Pharmacology, School of Medicine, University of California San Diego, La Jolla, California, USA [6]Service d'immunologie, Hôpital Robert Debré, AP-HP, Paris, France [7]EA3105, Université Paris Diderot, Paris, France [8]Service de microbiologie, Hôpital Robert Debré, AP-HP, Paris, France [9]Service de gastroentérologie, Hôpital Robert Debré, AP-HP, Paris, France

Correspondence to
Professor Jean-Pierre Hugot, INSERM U843, Hopital Robert Debré, 48 Boulevard Sérurier, 75019 Paris, France; jean-pierre.hugot@rdb.aphp.fr

Revised 7 July 2009
Accepted 14 July 2009
Published Online First 15 October 2009

ABSTRACT

Nucleotide oligomerisation domain 2 (*NOD2*) mutations are associated with susceptibility to Crohn's disease and graft-versus-host disease, two human disorders related with dysfunctions of Peyer's patches (PPs). In *Nod2*$^{-/-}$ mice transcellular permeability and bacterial translocation are increased in PPs. In this study, we show that both anti-CD4^{+} and anti-interferon γ (anti-IFNγ) monoclonal antibodies abrogate this phenotype and reduce the expression of tumour necrosis factor (TNF) receptor 2 and the long isoform of myosin light chain kinase, thus demonstrating that immune T cells influence the epithelial functions. In turn, intraperitoneal injection of ML-7 (a myosin light chain kinase inhibitor) normalises the values of CD4^{+} T cells, IFNγ and TNFα. This reciprocal cross-talk is under the control of the gut microflora as shown by the normalisation of all parameters after antibiotic treatment. Toll-like receptor 2 (TLR2) and TLR4 expression were increased in *Nod2*$^{-/-}$ mice under basal conditions and TLR2 and TLR4 agonists induced an increased transcellular permeability in *Nod2*$^{+/+}$ mice. Muramyldipeptide (a Nod2 agonist) or ML-7 was able to reverse this phenomenon. It thus appears that *Nod2* modulates the cross-talk between CD4^{+} T cells and the epithelium recovering PP and that it downregulates the pro-inflammatory effect driven by the ileal microflora, likely by inhibiting the TLR pathways.

INTRODUCTION

Caspase recruitment domain 15 (*CARD15*) also known as nucleotide oligomerisation domain 2 (*NOD2*) and NOD-LRR-CARD-2 (*NLRC2*) belongs to a family of genes involved in innate immunity.[1] Like toll-like receptors (TLR) *Nod2* is considered as a sensor of bacterial components. It can be activated by muropeptides, which are components of the bacterial cell wall. Nod2 signalling can interact with TLR signalling. Depending on the experimental conditions Nod2 may exert synergistic or inhibitory effects on TLR pathways.[2–5]

NOD2 polymorphisms have been associated with Crohn's disease,[6 7] a chronic relapsing inflammatory bowel disease (IBD) with mucosal ulcerations of the digestive tract.[8] In Crohn's disease, 30–50% of patients exhibit one or more *Nod2* genetic variations, which are usually considered as loss of function mutations. As a consequence, Crohn's disease is often seen as an immune deficiency towards bacteria present in the gut. However, the exact mechanisms by which *Nod2* mutations are able to induce Crohn's disease lesions are still subject to debate.

NOD2 has also been associated with mortality and graft-versus-host disease (GVHD) after bone marrow transplantation.[9 10] GVHD is associated with increased intestinal permeability and experimental models indicate that the primacy of gastrointestinal damage results in bacterial translocation followed by T cell activation and an increased cytokine release.[11 12] The incidence of severe GVHD rises from 18% in donor/recipient pairs without any *NOD2* variants to 37% in pairs with either donor or recipient mutations and 22–55% in pairs with both members mutated.[10 13] *NOD2* mutations seem to play a symmetric role in both donors and recipients, suggesting that NOD2 impairs function of both non-immune cells of the host and circulating immune cells of the graft.

Crohn's disease and GVHD lesions require gut-associated lymphoid formations known as lymphoid follicles (LFs).[14 15] LFs are encountered in the colon where they are isolated and in small bowel where they are grouped forming Peyer's patches (PPs). We have recently shown that *Nod2* invalidation in mice induces an hypertrophy and a hyperplasia of PPs after birth.[16] Crohn's disease and GVHD are characterised by a T helper 1 (Th-1) immune response with elevated rates of interferon γ (IFNγ) and tumour necrosis factor α (TNFα) in the mucosa.[17] In both disorders, the intestinal barrier is disrupted as shown by an excessive gut permeability of macromolecules and bacteria.[18 19] However, the link between Nod2 deficiency and the mucosal abnormalities observed in Crohn's disease or GVHD has not been fully explored. The aim of the present study was to dissect this link in a mouse model invalidated for NOD2.

MATERIAL AND METHODS

Animals and experimental protocols

C57BL/6 *Nod2*$^{+/+}$, *Nod2*$^{-/-}$ and *Nod2*$^{mut/mut}$ mutated mice were generated in the animal facility at Robert Debré Hospital.[16 20] All mice were housed in pathogen-free conditions with free access to food and water. Pathogen-free conditions were monitored every 6 months in accordance with the full set of FELASA high standards recommendations.

In vivo depletion of CD4^{+} Tcells was obtained by intraperitoneal injections of 100 µg purified GK1.5

(anti-L3T4 ($CD4^+$) monoclonal antibody (Pharmingen, Heidelberg, Germany) at both 96 and 24 h before experimentation.[21] For in vivo depletion of IFNγ, mice were intraperitoneally injected with 200 µg of a rat anti-mouse anti-IFNγ Ab XMG1.2 (Pharmingen) 24 h before experimentations.[22] Myosin light chain kinase (MLCK) inhibition was obtained by intraperotoneal injection twice daily of ML-7 (2 mg/kg; Sigma, Saint Quentin, France), a MLCK inhibitor, for 4 days before experiments.[23] Antibiotic protocols consisted in the administration of 1.0 g/l ampicillin and 0.5 g/l neomycin (Sigma) in drinking water for 12 days.[23]

Peyer's patches and spleen studies

Small intestine from *Nod2*$^{-/-}$ and *Nod2*$^{+/+}$ mice were removed and fixed in 4% phosphate-buffered formalin overnight. Samples were then stained with 0.5% methylene blue and decolourised in fresh 2% acid acetic. Then PP numbers were counted in a blind fashion.

Cell suspensions from PPs were prepared by pressing ileal PP with a syringe piston.[16] Cells from spleens were isolated using the same procedure with an additional step of erythrocyte lysis (Gey's solution). After centrifugation, cells were re-suspended in Dulbecco's modified Eagle's medium (DMEM) and submitted to flow cytometry analyses on a FACScalibur (Becton-Dickinson, Le Pont-de-Claix, France), and analysed by Cell Quest 3.3 (Becton Dickinson). Monoclonal antibodies used to stain cell suspensions were purchased from BD (Pharmingen): PE-Cy7-anti-CD3 (145-2C11), PE-Cy5-anti-CD4 (H129.19), fluorescein isothiocyanate (FITC)—anti-CD8 (53-6.7).

PPs and spleens from *Nod2*$^{+/+}$ and *Nod2*$^{-/-}$ mice were removed, and the concentration of proteins was determined using a commercial kit (Biorad, Marnes la Coquette, France). TNFα and IFNγ levels were determined by ELISA assays (BD Biosciences, Pharmingen, Hedelberg, Germany) according to the manufacturer's instructions.

Ussing chamber experiments

Biopsies from PPs were placed in a chamber exposing 0.196 cm^2 of tissue surface to 1.5 ml of circulating oxygenated Ringer solution at 37°C. PP transcellular permeability were assessed by measuring steady-state (from 1 to 2 h) mucosal-to-serosal flux of 40 kDa FITC—dextran (Sigma). Bacterial translocation was studied using chemically killed fluorescein-conjugated *Escherichia coli* or *Staphylococcus aureus* BioParticles (Molecular Probes, Leiden, The Netherlands) at a final concentration of 1.10^7 cfu/ml in the mucosal reservoir.

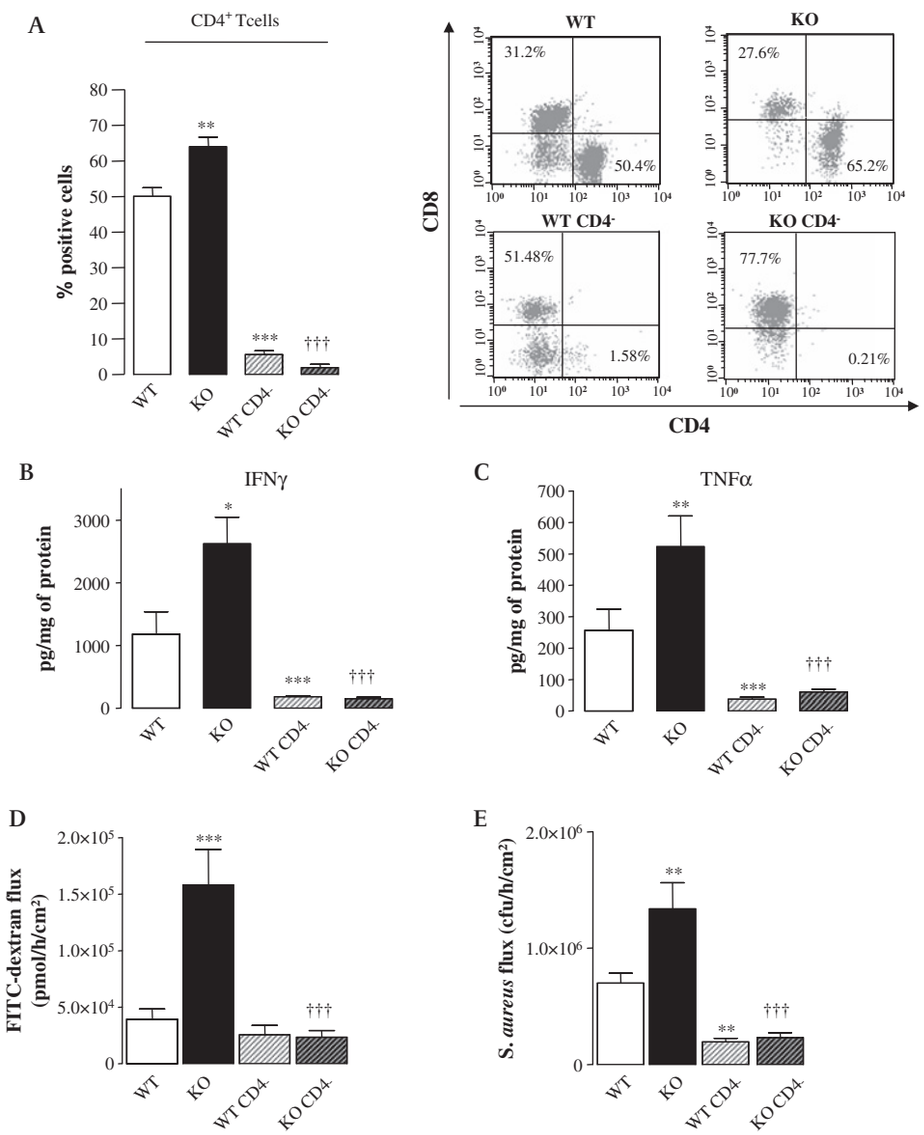

Figure 1 $CD4^+$ T cell depletion restores a normal phenotype of Peyers's patches (PPs) from *Nod2*$^{-/-}$ mice. Flow cytometry, ELISA and Ussing-chamber experiments were performed on PPs from *Nod2*$^{-/-}$ and *Nod2*$^{+/+}$ mice. (A) T cell composition of PPs. Each plot shows staining after gating on live $CD3^+$ T cells. (B and C) PP levels of interferon γ (IFNγ) and tumour necrosis factor α (TNFα). (D) Transcellular permeability was analysed by fluorescein isothiocyanate (FITC)—dextran flux. (E) Bacterial translocation of *Staphylococcus aureus*. Data represent the mean ± SEM of eight mice per group. *p <0.05, **p <0.01 and ***p <0.001, significantly different from *Nod2*$^{+/+}$ under basal conditions; ††p <0.01 and †††p <0.001, significantly different from *Nod2*$^{-/-}$ under basal conditions. KO, knock-out; WT, wild-type.

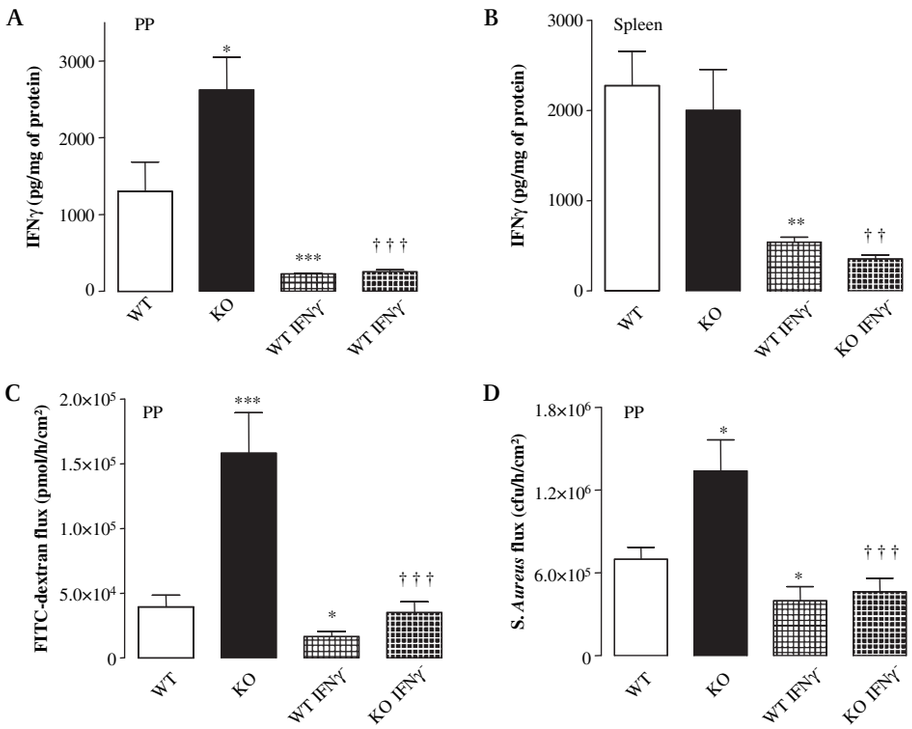

Figure 2 Interferon γ (IFNγ) contributes to disruption of the function of Peyer's patches (PPs) in *Nod2*$^{-/-}$ mice. ELISA and Ussing-chamber experiments were performed on PPs and spleens from *Nod2*$^{-/-}$ and *Nod2*$^{+/+}$ mice. (A and B) IFNγ levels in PPs and spleens. (C) Transcellular permeability was analysed by fluorescein isothiocyanate (FITC)—dextran flux. (D) Bacterial translocation of *Staphylococcus aureus*. Data represent the mean±SEM of eight mice per group. *p <0.05, **p <0.01 and ***p <0.001, significantly different from *Nod2*$^{+/+}$; ††p <0.01 and †††p <0.001, significantly different from *Nod2*$^{-/-}$ under basal conditions. KO, knock-out; WT, wild-type.

To investigate the role of TLR2/4 in the increase PP transcellular permeability, ultrapure and contaminant-free Pam3CSK4 (TLR2 agonist; Invivogen, Steinheim, Germany), PGN (TLR2 agonist; Fluka, San Diego, California, US) or lipopolysaccharide (LPS (TLR4 agonist; Sigma) were added into the luminal side of the Ussing chamber at final concentration 20 μg/ml. To investigate the effect of *Nod2* stimulation, mice were pre-treated intraperitoneally with MDP (100 μg/mouse/day; Sigma) for two consecutive days before experimentation and Ussing chamber experiments were performed after adding 10 μg/ml of MDP into the luminal side. For MLCK inhibition, mice were pre-treated by ML7 (see above) and 20 μg/ml of ML-7 were added in the Ussing chamber.

Measurement of in vivo transcellular permeability

Transcellular permeability was assessed by oral administration of fluorescein isothiocyanate-labelled dextran 40 kDa (FITC—dextran; Sigma). Mice were gavaged with FITC—dextran (12 mg/300 μl/mouse) 5 h prior to sacrifice. Whole blood FITC—dextran concentration was determined by a fluorimeter and transcellular permeability was expressed as the mean whole blood FITC—dextran concentration in ng/ml.

Immunohistochemistry of dendritic cells and apoptotic cells

PPs were removed and washed in cold phosphate-buffered saline (PBS), then samples were embedded in Tissue Tek medium (Euromedex, Souffelweyersheim, France). Cryostat sections (5 μm) were post-fixed with acetone (10 min, −20°C) and washed in PBS to eliminate Tissue Tek. Endogen peroxidases were blocked with 3% H_2O_2 (DAKO, Carpinteria, California, USA) and slides were incubated for 60 min with primary antibodies (purified hamster anti-mouse CD11C, dilution: 1/100; BD Pharmingen). A secondary antibody (anti-hamster) was then applied for 30 min, followed ABC kit (Vector Laboratories, Burlingame, California, USA) for 30 min. For detection, liquid 3,3′-diaminobenzidine (DAB) and Substrat (DAKO) was added for 10 min. Counts of positive CD11c cell in PPs were performed in a blind fashion.

After 2 h in the Ussing chamber, PPs were removed and washed in cold PBS. Then, PP samples were fixed in 4% phosphate-buffered formalin and embedded in paraffin blocks and cut into 5 μm sections. Briefly, 5 μm deparaffinised sections were subjected to a heat-induced antigen recovery in sodium citrate buffer solution pH 6. Endogen peroxidases were blocked with 3% H_2O_2 (DAKO) and slides were incubated for 30 min with primary antibodies (rabbit polyclonal antibody against cleaved caspase-3 (Asp 175, dilution: 1/100; Cell Signaling Technology, Ozyme, Beverly, Massachusetts, USA). A biotin-labelled secondary antibody was then applied for 30 min, followed by avidin—biotin—peroxidase conjugate for 30 min (Vector Laboratories). For detection, peroxidase enzyme substrate 3,3′-diaminobenzidine was added to yield a brown reaction product. The slides were counterstained with Harris haematoxylin. Counts of positive caspase-3-cleaved cells in PPs were performed in a blind fashion.

Ileal bacterial counts

Ileum was removed and ileal content was collected using sterile water (Biorad). Then, ileal content was homogenised and serial dilutions of each aliquot (50 μl) were plated onto five selective gelose plates (URI 4, Drigalski, Columbia ANC + 5% of sheep blood, Chapman and Coccosel). Plates were incubated for 24 h at 37°C under aerobic condition and the number of colony forming units was counted and expressed as cfu/mg of ileal content.

Real time reverse transcription-polymerase chain reaction

After extraction by the NucleoSpin RNA II Kit (Macherey-Nagel, Hoerdt, France), total RNAs were converted to cDNA using random hexonucleotides and then used for RT-PCR. We conducted PCR with QuantiTect SYBR Green PCR Kit (Applied, Courtaboeuf, France) using sense and antisense primers specific for G3PDH, the long MLCK isoform (specifically expressed by epithelial cells), tumour necrosis factor receptor 1 (TNFR1), TNFR2, TLR2 and TLR4 (sequence are shown in supplementary table 1). After amplification, we determined the threshold cycle (Ct) to obtain expression values of $2^{-\Delta Ct}$.

Statistical analyses

Values are expressed as mean ± SEM. Statistical analysis were performed using GraphPad Prism 4.00 software package for PC. Comparisons were performed by the unpaired Student t test. A value of $p < 0.05$ was considered as statistically significant.

RESULTS

$CD4^+$ T cells and IFNγ trigger PP barrier dysfunction in *Nod2*$^{-/-}$ mice

As previously reported,[16] $CD4^+$ T–cells were increased in the PPs of *Nod2*$^{-/-}$ mice (figure 1A). In order to define their role, *Nod2*$^{+/+}$ and *Nod2*$^{-/-}$ mice were treated with anti-$CD4^+$ antibodies. $CD4^+$ T cell depletion was effective in both PPs and spleen as shown in figure 1A and supplementary figure 1A. It was associated with a decrease of IFNγ and TNFα tissue concentration (figure 1B,C and supplementary figure S1B,C). Similarly, $CD4^+$ T cells abrogated the increase of PP transcellular permeability as well as *S aureus* translocation in *Nod2*$^{-/-}$ mice (figure 1D,E). In addition, after $CD4^+$ T cell depletion these parameters were similar in *Nod2*$^{+/+}$ and *Nod2*$^{-/-}$ mice (figure 1D,E). We thus concluded that $CD4^+$ T cells play a major role in the whole phenotype observed in case of Nod2 deficiency.

$CD4^+$ T cells are known to produce IFNγ which is a key factor in the Th1 response and we have previously shown that IFNγ levels are increased in *Nod2*$^{-/-}$ mice.[16] In order to test the role of IFNγ on the phenotype, we then treated mice with anti-IFNγ antibodies. In PPs and spleen, IFNγ concentrations measured by ELISA methods, were dramatically reduced in both *Nod2*$^{-/-}$ and *Nod2*$^{+/+}$ mice (figure 2A,B). In parallel, the transcellular permeability and the bacterial ingress were also decreased in PP from *Nod2*$^{-/-}$ mice (figure 2C,D). A similar but less dramatic effect was observed in *Nod2*$^{+/+}$ mice (figure 2C,D). As a result, after IFNγ depletion, epithelial permeability and bacterial translocation rates were similar in *Nod2*$^{-/-}$ and *Nod2*$^{+/+}$ mice. Thereby IFNγ modulate the intestinal function in *Nod2*$^{-/-}$ mice.

In other animal models, IFNγ and T cells have been reported to disrupt epithelial barrier integrity by upregulating TNFR2 and MLCK expression.[23 24] We thus investigated the mRNA expression of TNFR1, TNFR2 and MLCK. Under basal condition and after $CD4^+$ or IFNγ depletion, no significant differences were shown for TNFR1 mRNA expression in PPs (figure 3A). In contrast, an increased expression of TNFR2 and the long isoform of MLCK were seen in *Nod2*$^{-/-}$ mice compared to controls (figure 3B,C). After $CD4^+$ or IFNγ depletion, TNFR2 mRNA expression decreased in PP from *Nod2*$^{+/+}$ and *Nod2*$^{-/-}$ mice with a normalisation of TNFR2 mRNA expression in *Nod2*$^{-/-}$ mice. IFNγ or $CD4^+$ depletions were able to reverse this phenotype while they did not affect MLCK expression in *Nod2*$^{+/+}$ mice. We thus concluded that $CD4^+$ and IFNγ modulate the MLCK expression in epithelial cells recovering PPs.

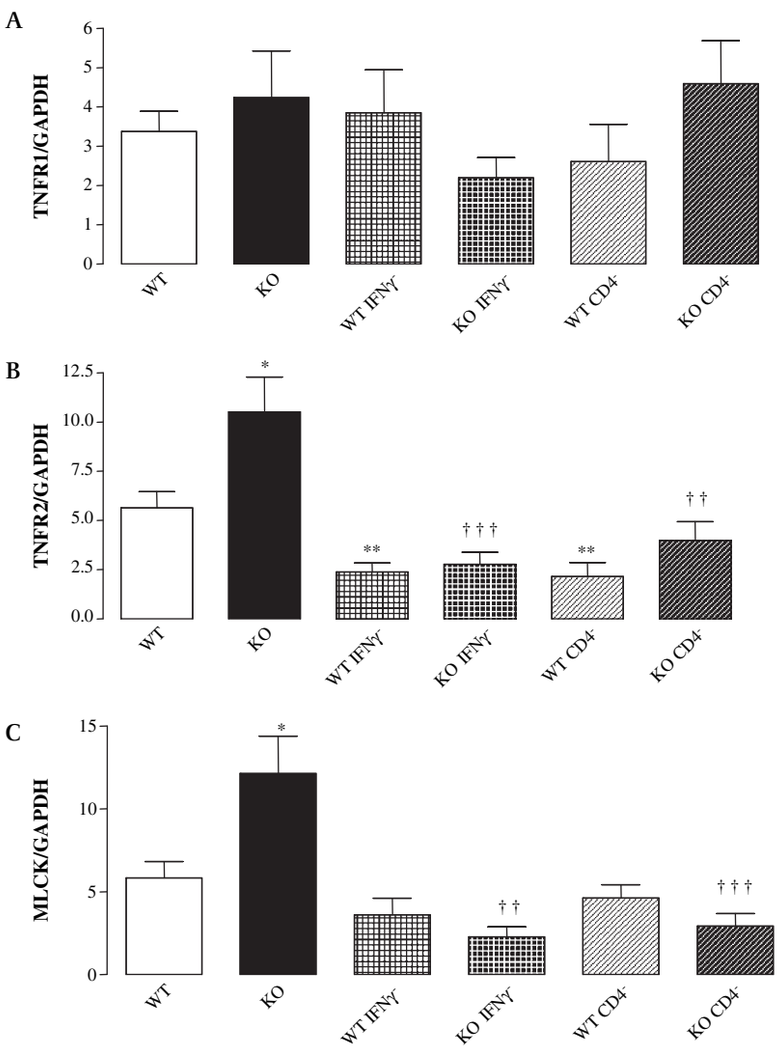

Figure 3 $CD4^+$ T cells and IFNγ depletion abrogate the increased mRNA expression of TNFR2 and MLCK in PPs from *Nod2*$^{-/-}$ mice. Real-time PCR experiments were performed on PPs from *Nod2*$^{-/-}$ and *Nod2*$^{+/+}$ mice. (A–C) TNFR1, TNFR2 and MLCK mRNA expression. Data represent the mean±SEM of eight mice per group. *$p < 0.05$ and **$p < 0.01$ significantly different from *Nod2*$^{+/+}$ under basal conditions; $^{\dagger\dagger}p < 0.01$ and $^{\dagger\dagger\dagger}p < 0.001$, significantly different from *Nod2*$^{-/-}$ under basal conditions. IFNγ, interferon γ; KO, knock-out; MLCK, myosin light chain kinase; PCR, polymerase chain reaction; PPs, Peyer's patches; TNFR, tumour necrosis factor receptor. WT, wild-type.

Epithelial MLCK is involved in PP homeostasis in *Nod2*$^{-/-}$ mice

As MLCK has been reported to disrupt the epithelial integrity[23–25] we further investigated its role by treating the animals with ML-7, a MLCK inhibitor. In *Nod2*$^{+/+}$ mice, ML-7 slightly reduced the ingress of *S aureus* through the epithelium recovering PP while it did not affect the transcellular permeability as well as the bacterial passage of *E coli* (figure 4A–C). In contrast, in *Nod2*$^{-/-}$ mice, the PP permeability and the bacterial ingresses (*E coli* and *S aureus*) were dramatically reduced by ML-7 treatment with a normalisation of these parameters compared to control mice. We concluded that MLCK plays a key role in the observed epithelial dysfunction in *Nod2*$^{-/-}$ mice.

We further explored the impact of the observed epithelial abnormalities on the mucosal inflammation. ML-7 treatment decreased the percentage of CD4$^+$ T cells in *Nod2*$^{-/-}$ mice while it did not affect the cellular composition in *Nod2*$^{+/+}$ mice (figure 5A). Indeed, after ML-7 treatment, PP from *Nod2*$^{+/+}$ and *Nod2*$^{-/-}$ mice exhibited similar rates of CD4$^+$ T cells. In comparison, ML-7 treatment did not change the T cell composition in spleen (supplementary figure S2). Comparable results were obtained in terms of cytokine levels in the PPs. ML-7 treatment did not modify the IFNγ and TNFα levels in *Nod2*$^{+/+}$ mice (figure 5B,C). In contrast, it decreased IFNγ and TNFα tissue concentrations in *Nod2*$^{-/-}$ mice, turning these values to normal ranges. Here too, ML-7 did not affect the studied parameters in the spleen (supplementary figure S2). Finally, ML-7 decreased and restored a normal expression of TNFR2 and MLCK but did not change TNFR1 mRNA expression in PP from *Nod2*$^{-/-}$ mice (figure 5D–F). Consequently, we concluded that MLCK plays a major role in the PP phenotype of *Nod2*$^{-/-}$ mice.

Antibiotic treatment reverses the phenotype of *Nod2*$^{-/-}$ mice

Crohn's disease and GVHD lesions are related to an abnormal response of the host towards bacteria. We thus analysed the role of the gut microflora in the observed phenotype. Both *Nod2*$^{+/+}$ and *Nod2*$^{-/-}$ mice were treated by antibiotics (ABTs). ABT treatment almost totally suppressed the aerobic microflora and only a small population of *Staphylococcus* spp. persisted at a comparable level in *Nod2*$^{+/+}$ and *Nod2*$^{-/-}$ mice (supplementary table 2). While treatment with ABTs did not change the number of PP in *Nod2*$^{+/+}$ mice, it significantly decreased the number of PP in *Nod2*$^{-/-}$ mice (figure 6A). In addition, ABTs reduced the number of immune cells per PP in *Nod2*$^{-/-}$ and *Nod2*$^{+/+}$ mice (figure 6B). In contrast, the number of splenocytes was not affected by ABT treatment in either mice strain (supplementary figure S3).

ABT strongly reduced the percentage of CD4$^+$ T cells in PPs of both *Nod2*$^{+/+}$ and *Nod2*$^{-/-}$ mice (figure 6C) demonstrating that the ileal microflora modulates the percentage of CD4$^+$ T cells in PPs. In contrast, ABTs did not alter the percentage of CD4$^+$ T cells in spleens from *Nod2*$^{+/+}$ and *Nod2*$^{-/-}$ mice (supplementary figure S3). ABTs also decreased the levels of IFNγ and TNFα in PPs of *Nod2*$^{-/-}$ mice (figure 6D,E). In parallel, in PPs from *Nod2*$^{-/-}$ ABTs decreased TNFR2 and MLCK mRNA expression (figure 7A–C). They reduced the permeability and bacterial passage through PPs (figure 7D–F).

Together these results show that suppression of the intestinal microflora is able to fully reverse the phenotype of *Nod2*$^{-/-}$ mice. In contrast, ABT treatment had only limited effects on the PP phenotype of *Nod2*$^{+/+}$ mice and no changes were observed in the spleen of both mouse strains after ABT (supplementary figure S3). Finally, comparable results were obtained when using ABT protocols containing metronidazole (antibiotic spectrum against anaerobic bacteria) in addition to ampicillin and neomycin (data not shown).

Nod2 downregulates the increased PP permeability driven by TLR2/4 agonists

Nod2 plays a crucial role in the immune tolerance to bacteria by decreasing the production of inflammatory cytokines in response to TLR2/4.[2 3 5] Consequently, we investigated whether this negative cross-talk between TLR and NOD2 may contribute to the increased permeability observed in PP from *Nod2*$^{-/-}$ mice.

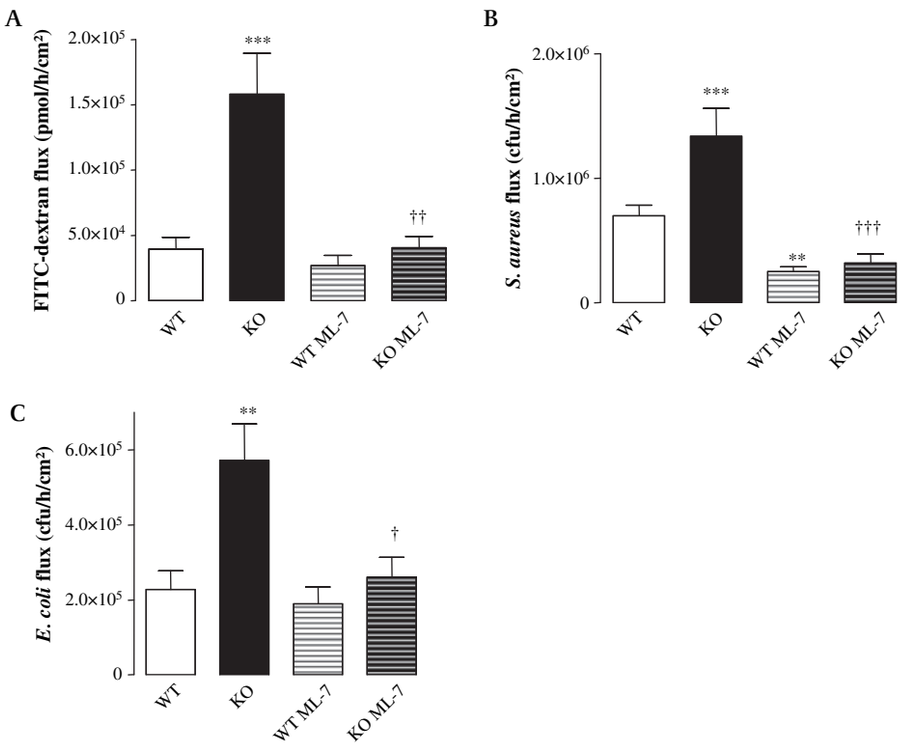

Figure 4 MLCK participates in the disruption of PP function in *Nod2*$^{-/-}$ mice. Ussing-chamber experiments were performed on PPs from *Nod2*$^{-/-}$ and *Nod2*$^{+/+}$ mice. (A) Transcellular permeability was analysed by FITC–dextran flux. (B and C) Bacterial translocation of *Staphylococcus aureus* or *Escherichia coli*. Data represent the mean±SEM of eight mice per group. **p <0.01 and ***p <0.001, significantly different from *Nod2*$^{+/+}$ under basal conditions; †p <0.05, ††p <0.01 and †††p <0.001, significantly different from *Nod2*$^{-/-}$ under basal conditions. FITC, fluorescein isothiocyanate; KO, knock-out; MLCK, myosin light chain kinase; PPs, Peyer's patches. WT, wild-type.

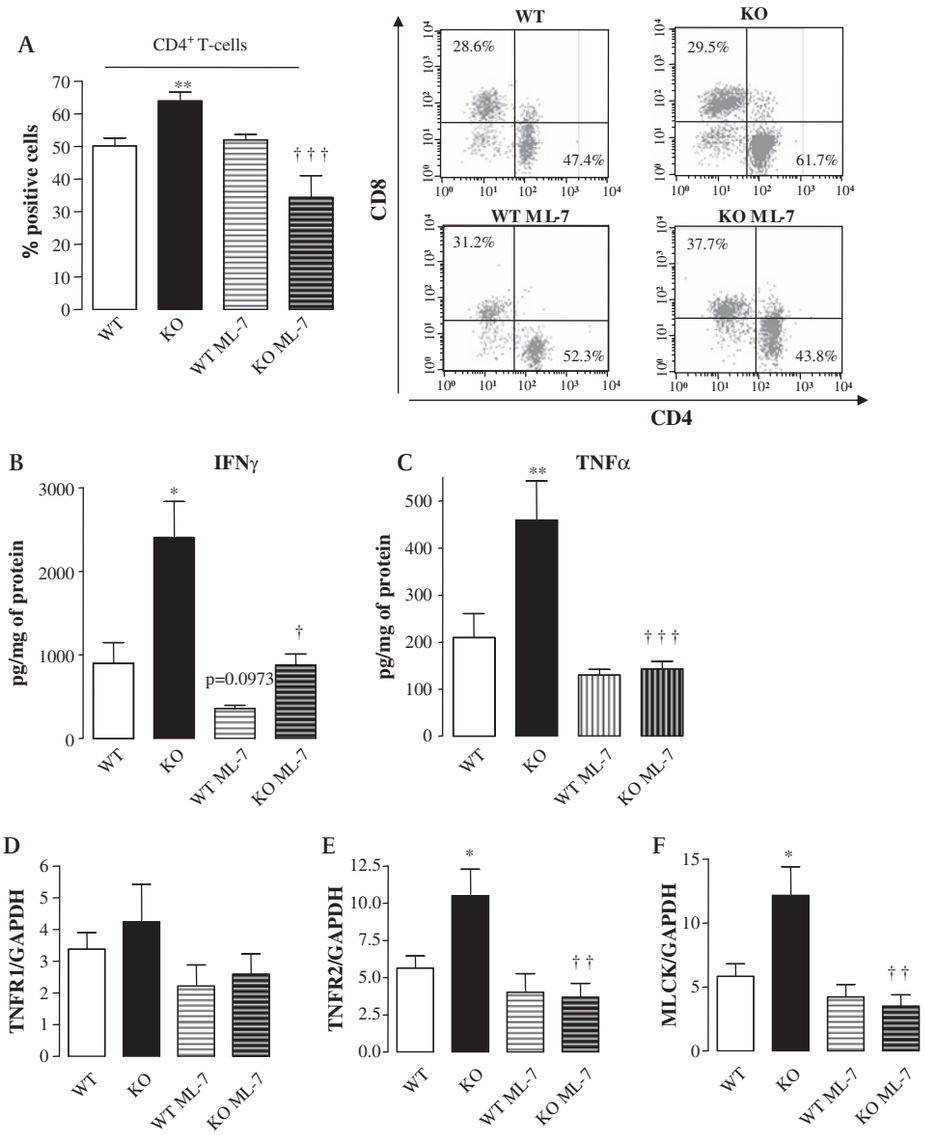

Figure 5 MLCK is involved in the regulation of PP homeostasis in *Nod2*$^{-/-}$ mice. Flow cytometry, ELISA and real-time PCR experiments were performed on PPs from *Nod2*$^{-/-}$ and *Nod2*$^{+/+}$ mice. (A) T cell composition was investigated using antibodies to CD3, CD4, CD8. Each plot shows staining after gating on live CD3^{+} T cell. (B and C) Levels of IFNγ and TNFα. (D–F) TNFR1, TNFR2 and MLCK mRNA expression. Data represent the mean±SEM of eight mice per group. *p <0.05 and **p <0.01, significantly different from *Nod2*$^{+/+}$ under basal conditions; †p <0.05, ††p <0.01 and †††p <0.001 significantly different from *Nod2*$^{-/-}$ under basal conditions. IFNγ, interferon γ; KO, knock-out; MLCK, myosin light chain kinase; PPs, Peyer's patches; TNFα, tumour necrosis factor α; TNFR, TNF receptor; WT, wild-type.

Under basal condition, PP from *Nod2*$^{-/-}$ mice exhibited an increased mRNA expression of TLR2 and TLR4 in comparison with controls (figure 8A,B). CD4^{+} depletion, IFNγ depletion, ABT treatment or ML-7 treatment were all able to decrease TLR2 and TLR4 expressions in PP from *Nod2*$^{-/-}$ mice, while they had only a limited effect in *Nod2*$^{+/+}$ mice. This observation suggests that TLR2 and TLR4 over-expression in *Nod2*$^{-/-}$ mice is secondary to the abnormal PP phenotype. Next, we studied the effect of agonists for TLR2 (Pam3CSK4 and PGN) and/or TLR4 (purified LPS) on PP permeability. These molecules do not alter the number of apoptotic cells of PPs mounted in Ussing chambers (supplementary figure S5). Any of the studied TLR agonists increased the transcellular permeability of the PPs from *Nod2*$^{+/+}$ mice while they did not alter the permeability of *Nod2*$^{-/-}$ mice (figure 8C). This effect was abrogated when the *Nod2*$^{+/+}$ mice were pre-treated with MDP or ML7 (figure 8C). Altogether, these observations showed that TLR stimulation alters the PP permeability through the MLCK pathway and that *Nod2* downregulates this effect.

Previous reports suggest that TLR2/4 activation enhances transepithelial transport of microparticles by M cells and migration of subepithelial dendritic cells (DCs) into the follicle-associated epithelium (FAE).[26] Although PPs from *Nod2*$^{-/-}$ exhibited a similar number of DCs than *Nod2*$^{+/+}$ mice,[16] we therefore investigated the distribution of DCs in PPs. In vivo, no differences were observed between *Nod2*$^{+/+}$ and *Nod2*$^{-/-}$ mice for the distribution of DCs into the FAE and in the subepithelial compartment of PPs (supplementary figure S4A–D). However, after ex vivo TLR stimulation in Ussing chambers, there was an increased number of DCs into the FAE in comparison with unstimulated PPs as previously reported (supplementary figure S4E,F).

Role of bacterial translocation through Peyer's patches in *Nod2* animal models

The main phenotype investigated in this work consists in the translocation of bacteria through PP formations. However, the role of the ileal mucosa beside the PP structures is questionable. We have previously shown that out of PP areas, the bacterial translocation of *E coli* was low and that it was not altered in *Nod2*$^{-/-}$ mice.[16] As a result, we concluded that the role of the ileal mucosa out of LF structures seems to be limited in terms of bacterial translocation. However, it is of note that in the ileum outside the PPs, the transcellular permeability was increased in

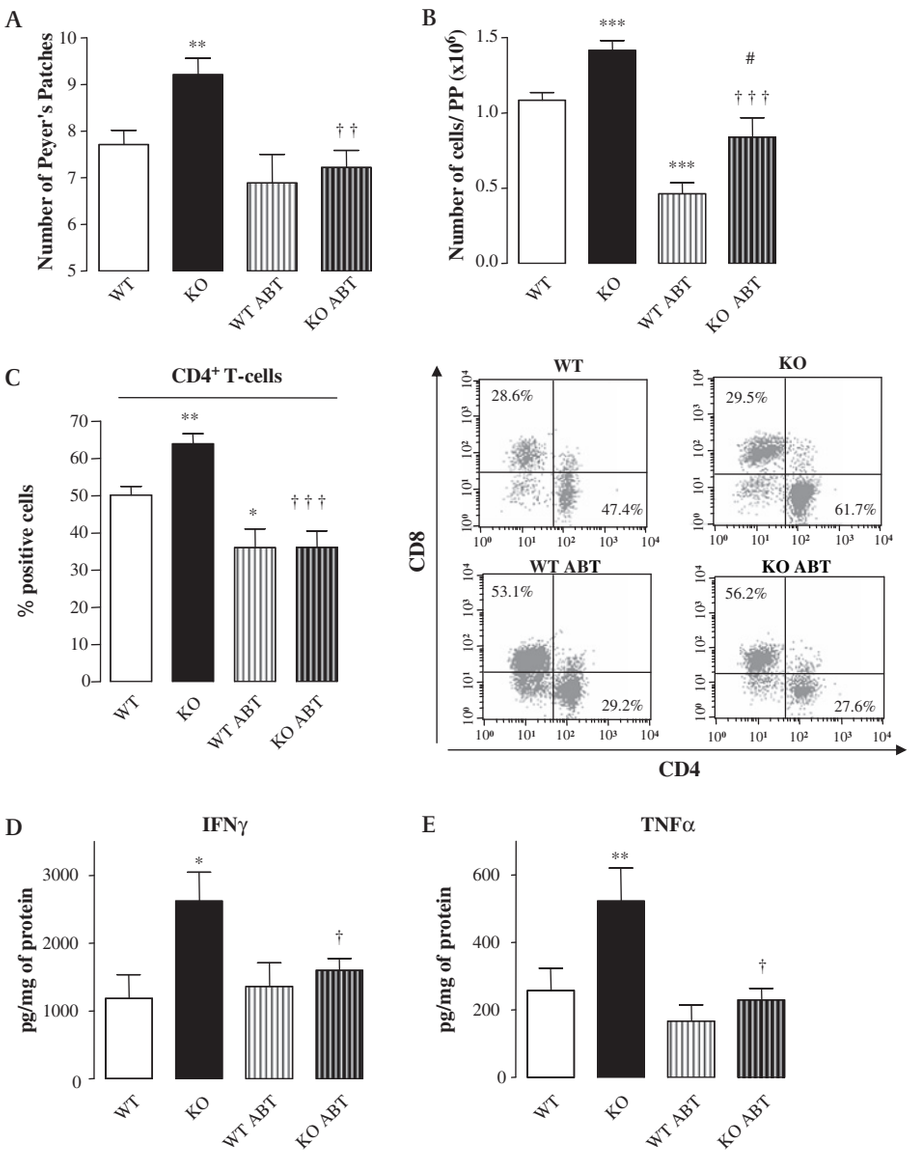

Figure 6 Ileal microflora disrupt PP homeostasis in *Nod2*$^{-/-}$ mice. (A) PP count on the whole intestines of *Nod2*$^{-/-}$ and *Nod2*$^{+/+}$ mice. (B) Number of immune cells per PP in basal conditions and after ABTs. (C) T cell composition of PPs was investigated using antibodies to CD3, CD4 and CD8. Each plot shows staining after gating on live CD3^{+} T cells. (D and E) Levels of IFNγ and TNFα. Data represent the mean±SEM of eight mice per group. *p <0.05, **p <0.01 and ***p <0.001, significantly different from WT under basal conditions; †p <0.05, ††p <0.01 and †††p <0.001, significantly different from *Nod2*$^{-/-}$ under basal conditions and; $^{\#}$p <0.05 significantly different *Nod2*$^{+/+}$ after ABTs. ABTs, antibiotics; IFNγ, interferon γ; KO, knock-out; PPs, Peyer's patches; TNFα, tumour necrosis factor α; WT, wild-type.

Nod2$^{-/-}$ mice. This phenotype was reversed by oral ABT (figure 9A). In consequence, it is not possible to rule out a role in antigen transport of the ileum out of the PP areas. In addition, the effect of Nod2 deficiency on the paracellular transport has not been studied and it will require further investigations.

Because our data have been obtained almost exclusively in Ussing chamber experiments, we wanted to confirm the ex vivo increased bacterial translocation in *Nod2*$^{-/-}$ mice by in vivo methods. For this reason, we used the FITC-labelled dextran 40 kDa (FITC–dextran) as a non-metabolisable trans-cellular permeability probe. After oral ingestion, the fluorescent particle was recovered at a higher rate in the blood of *Nod2*$^{-/-}$ mice demonstrating the relevance of our findings in vivo (figure 9B).

Finally, because Crohn's disease and GVHD are associated with Nod2 mutations rather than *NOD2* deletion, we looked at the phenotype of the previously described *Nod2*$^{mut/mut}$ mice carrying a frame-shift mutation homologous to the Crohn·s disease associated 1007fs human mutation.[27] Like *Nod2*$^{-/-}$ mice, *Nod2*$^{mut/mut}$ mice exhibited an increased number of PPs and an increased number of immune cells per PP (figure 9C and D). In addition, *Nod2*$^{mut/mut}$ mice were also characterised by an elevated translocation of *E coli* in Ussing chamber experiments (figure 9E).

DISCUSSION

Despite a well-established association between *NOD2* mutations and Crohn·s disease[6 7] as well as GVHD,[9 10] the mechanisms by which NOD2 mutations induce these diseases in human are poorly understood. Because Crohn·s disease and GVHD have been related to host–microbial interactions and because alterations of PPs have been shown in both diseases,[14 15] we focused on these specialised GALT formations. We have previously shown that deletion of Nod2 in mice causes alterations of the structure and the permeability of PP.[16] Here we show that these alterations result from an impaired interaction between immune and epithelial cells implicating CD4^{+} T cell infiltration, IFNγ secretion and MLCK activity in epithelial cells recovering PPs. This PP dysfunction is under the control of the ileal microflora and it may be reproduced by TLR2/4 stimulation. Altogether, these data suggest that *Nod2* contributes to the immunogenic tolerance towards gut microflora likely by down-regulating the TLR pathways. A schematic representation of the

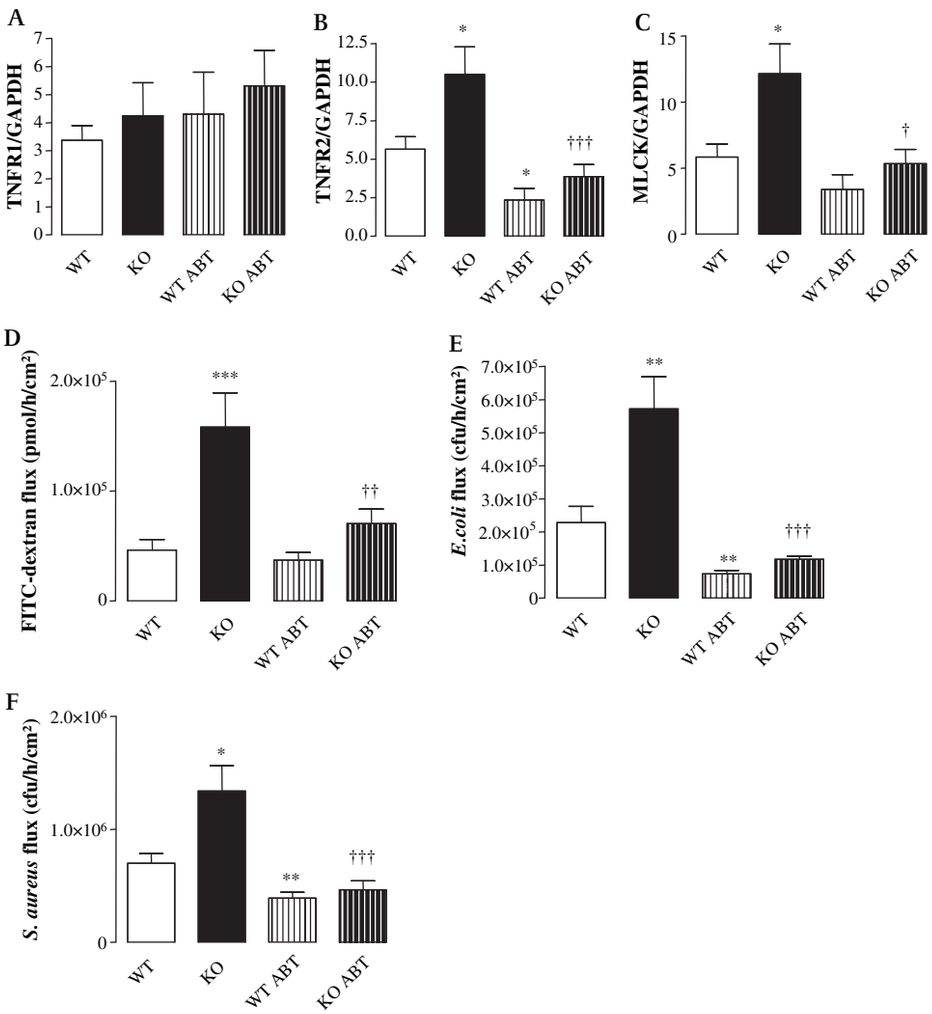

Figure 7 Ileal microflora alters TNFR2 and MLCK expression and changes PP function in *Nod2*$^{-/-}$ mice. Real-time PCR and Ussing-chamber experiments were performed on PPs from *Nod2*$^{-/-}$ and *Nod2*$^{+/+}$. (A–C) TNFR1, TNFR2 and MLCK mRNA expression. (D) Transcellular permeability were analysed by FITC–dextran flux in PPs. (E and F) Translocation of *Staphylococcus aureus* and *Escherichia coli*. Data represent the mean±SEM of eight mice per group. *p <0.05, **p <0.01 and ***p <0.001, significantly different from *Nod2*$^{+/+}$ under basal conditions; †p <0.05, ††p <0.01 and †††p <0.001, significantly different from *Nod2*$^{-/-}$ under basal conditions. ABT, antibiotic; FITC, fluorescein isothiocyanate; GAPDH, glyceraldehyde-3-phosphate dehydrogenase; KO, knock-out; MLCK, myosin light chain kinase; PPs, Peyer's patches; TNFR, tumour necrosis factor receptor; WT, wild-type.

proposed interactions is shown in the supplementary figure S6. Finally, the preliminary data obtained on the mouse model carrying the mutation homologous to the human frame-shift mutation suggest that the proposed model may be relevant for Crohn·s disease-associated mutations.

Commensal bacteria play a critical role in the postnatal development and maintenance of the gut-associated lympoid tissue (GALT).[28 29] Germ-free animals have an underdeveloped GALT and are resistant to colitis and GVHD. TLRs and NODs have been considered as putative key factors of GALT development under the stimulation the resident flora. TLRs play only a limited role in the postnatal development of PP.[30] We have previously reported that *Nod2*$^{-/-}$ mice exhibit a hyperplasia and a hypertrophy of the GALT after birth, suggesting an important role of *Nod2* in the development of GALT during the bacterial colonisation of gut.[16] This pivotal role has been herein reinforced by the fact that the *Nod2* mutated mice (namely *Nod2*$^{mut/mut}$) also exhibit a hyperplasia and a hypertrophy of the PP with a concomitant elevated translocation of *E coli*. As this now shows that the deletion of the intestinal flora by oral ABT reverses this phenotype, we conclude that *Nod2* downregulates the development of the GALT induced by the gut microflora.

It has been shown that the gut microflora drive the expansion of proinflammatory CD4$^+$ T cells in the colonic lamina propria under normal and inflammatory conditions.[31] Moreover, Yaguchi *et al* have shown that treatment of *Nod2*$^{+/+}$ mice with by subcutaneous injections of antibiotics decreases the numbers of lymphocytes in PP without significant changes in the lymphocyte phenotype and cytokine levels.[32] In agreement with this study, we found that oral ABT reduce the number of T cells in PPs from *Nod2*$^{+/+}$ mice without changes in their cytokine contents but, in contrast, we found that oral ABT reduced the percentage of CD4$^+$ T cells. This limited discrepancy could be explained by differences in ABT regimens, our ABT protocol being longer and more efficient to destroy ileal microflora.

In the absence of *Nod2*, gut microflora exert a stronger stimulation on the PPs as shown by a higher proportion of CD4$^+$ T cells, higher levels of inflammatory cytokines and, finally, higher permeability rates for antigens and bacteria. All of these alterations were suppressed after treatment with oral antibiotics. As a result, *Nod2* appears not only to influence the development of the GALT but it is also able to modulate the immune response towards bacteria, by limiting the development of a Th1 immune response. These results are in agreement with data showing that NOD2 activation in DCs regulates their ability to induce a polarised Th1 response in CD4$^+$ T cells.[33] In *NOD2*$^{+/+}$ DCs, MDP acts synergistically with lipopolysaccharide (LPS) to promote the proliferation of naïve CD4$^+$ T cells with a Th2-like cytokine profile. By contrast, DCs carrying *NOD2* mutations are unable to react to MDP, but they respond to LPS and they promote the development of Th1-orientated cells. As a consequence, patients with Crohn·s disease who are NOD2 deficient are predisposed to the generation of strongly polarised Th1 response against commensal microorganisms.[33]

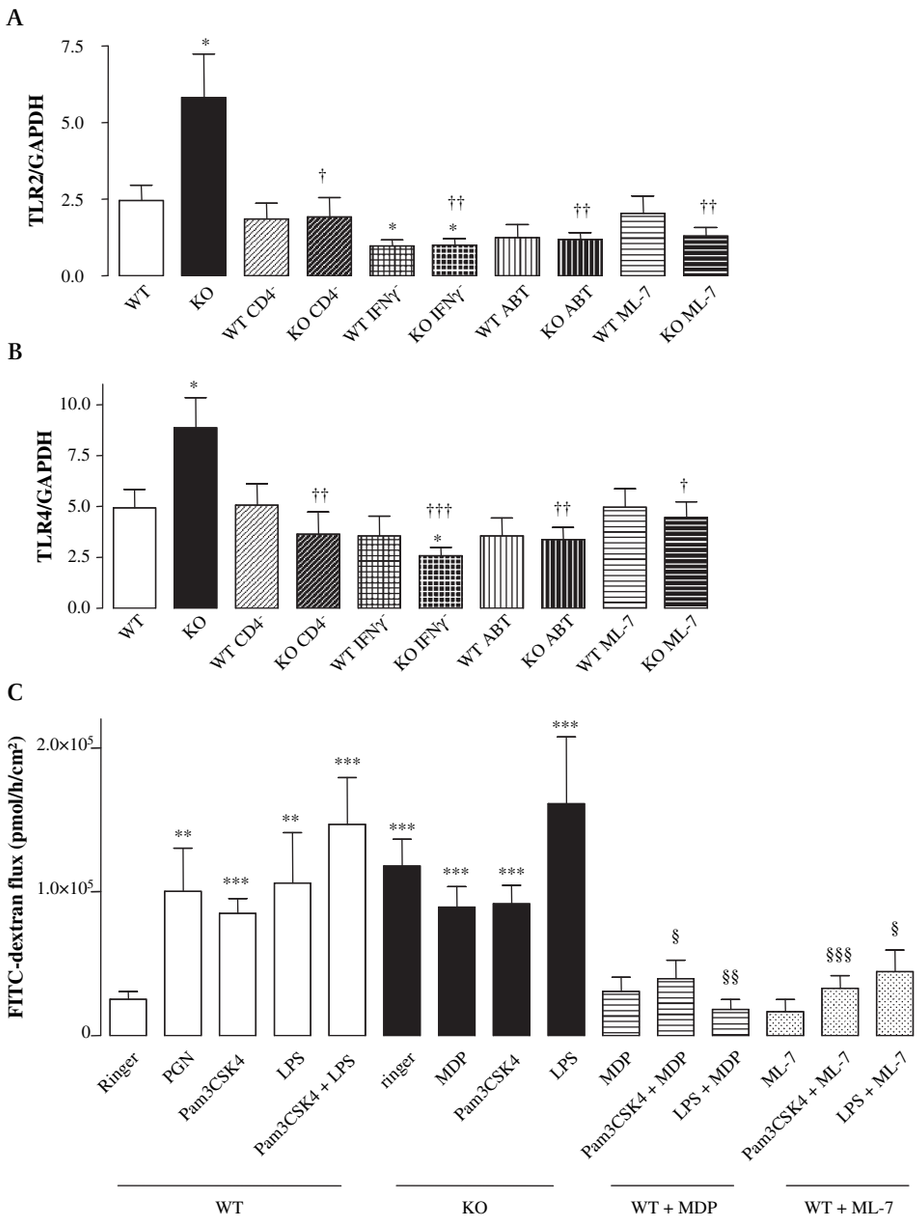

Figure 8 *Nod2* downregulates the effect of TLR2/4 agonists on transcellular permeability. (A and B) TLR2 and TLR4 mRNA expressions in PPs from *Nod2*$^{-/-}$ and *Nod2*$^{+/+}$. (C) Transcellular permeability were analysed by FITC–dextran flux. PP from *Nod2*$^{+/+}$ and *Nod2*$^{-/-}$ mice were mounted in Ussing chambers and Pam3CSK4, PGN, LPS, ML-7 or MDP were added into the luminal side. To investigate the roles of *Nod2* and MLCK, *Nod2*$^{+/+}$ mice were respectively treated with MDP or ML-7 before experiments. Data represent the mean±SEM of eight mice per group. **p <0.01 and ***p <0.001, significantly different from *Nod2*$^{+/+}$ under basal condition; §p <0.05, §§p <0.01 and §§§p <0.001, significantly different from *Nod2*$^{+/+}$ treated by TLR2 or TLR4 agonist. ABT, antibiotic; FITC, fluorescein isothiocyanate; KO, knock-out; LPS, lipopolysaccharide; MDP, muramyl dipeptide; MLCK, myosin light chain kinase; PGN, peptigoglycan; PPs, Peyer's patches; TLR, toll-like receptor; WT, wild-type.

CD4^{+} T cells play a pivotal role in the pathogenesis of human inflammatory diseases as well as experimental colitis.[34 35] Interleukin 2 knock-out (IL2 KO) mice develop spontaneous intestinal inflammation which requires CD4^{+} T cells.[36] The transfer of CD45Rb^{high} CD4^{+} T cell into SCID mice induces an intestinal inflammation.[37] Finally, immunotherapy with anti-CD4 may be of benefit in IBD.[38] In agreement, we show here that CD4^{+} depletion fully reverses the phenotype observed in *Nod2*$^{-/-}$ mice. In Crohn·s disease and other intestinal diseases with compromised barrier function, the Th1 immune activation is associated with increased levels of mucosal IFNγ and TNFα. In vitro studies have shown that IFNγ and TNFα induced barrier dysfunction in cultured epithelial monolayers.[39 40] Finally, in human and in animal models, IFNγ and TNFα antagonists can diminish disease severity and restore barrier function.[23 41–43] In agreement with these observations, our data show that IFNγ overexpression in *Nod2*$^{-/-}$ mice plays a key role in the disruption of the epithelial barrier integrity of PPs. In addition, it has been shown that IFNγ primes the intestinal epithelium to respond to TNFα by inducing TNFR2 expression, which in turn mediates TNFα-induced MLCK-dependent barrier dysfunction.[24] In accordance with these findings, we found that TNFR2 and MLCK mRNA expression are dependent on IFNγ secretion in our model. During the last decade, growing evidence has pointed to the crucial role of MLCK in the barrier dysfunction observed in the pathogenesis of gut inflammation.[25] MLCK expression and activity are upregulated in ileal and colonic areas involved in IBD and the degree of upregulation correlates positively with the degree of active inflammation.[25] In addition, MLCK is involved in LPS-induced disruption of colonic epithelial barrier and bacterial translocation in rats[44] as well as in the barrier dysfunction induced by TNFα.[45 46]

Here we show that PPs from *Nod2*$^{-/-}$ mice exhibit an increased expression of the long isoform of MLCK. This isoform, specifically expressed by gut epithelial cells and endothelial cells, is responsible of MLC phosphorylation which modulates the intestinal permeability.[47] More importantly, the inhibition of MLCK activity by ML-7 treatment was able to completely reverse the mucosal phenotype in PPs from *Nod2*$^{-/-}$ mice

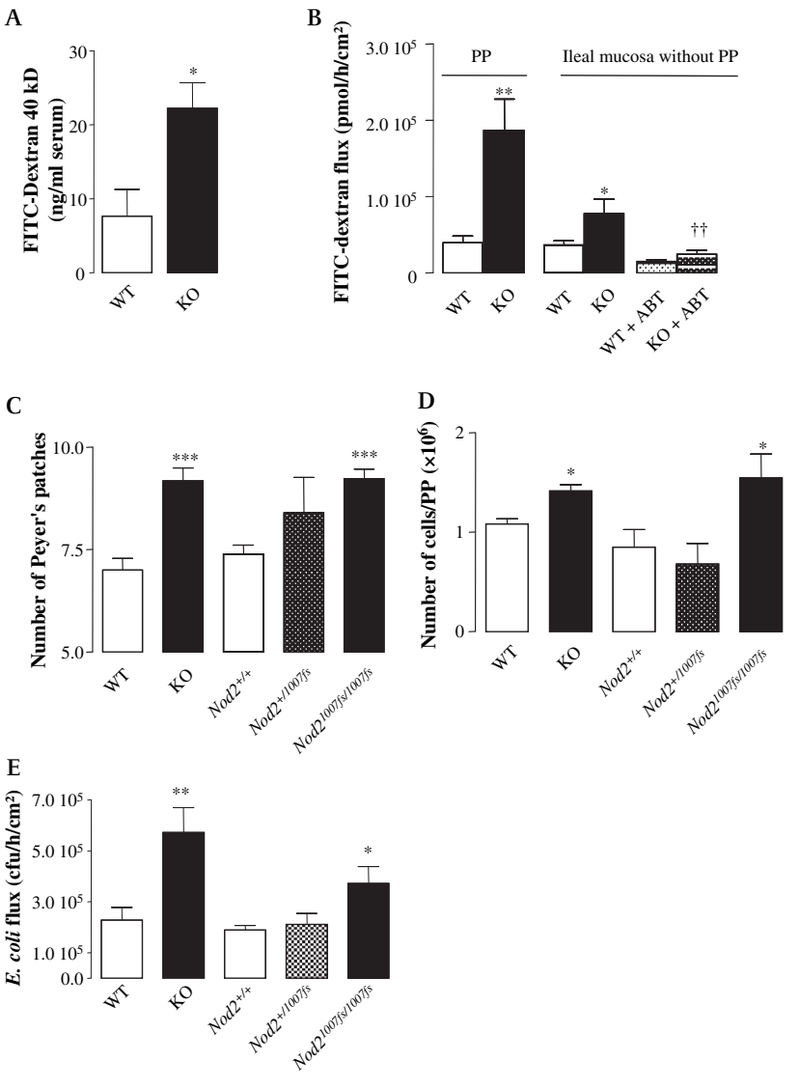

Figure 9 Role of bacterial translocation through PPs in *Nod2* animal models. (A) Transcellular permeability was analysed by FITC–dextran 40 kDa flux through PPs and ileal mucosa free of PPs. (B) In vivo transcellular permeability analyses: FITC–dextran 40 kDa was measured in serum from $Nod2^{+/+}$ and $Nod2^{-/-}$ mice recovered after oral inoculation of the macromolecule. (C) PP counts in the whole intestines of $Nod2^{mut/mut}$, $Nod2^{snp13/+}$ and $Nod2^{+/+}$ mice. (D) Number of immune cells per PP under basal conditions. (E) Bacterial translocation of *Escherichia coli* through PP formations. Data represent the mean±SEM of at least eight mice per group. *p <0.05, **p <0.01 and ***p <0.001, significantly different from $Nod2^{+/+}$. FITC, fluorescein isothiocyanate; KO, knock-out; PPs, Peyer's patches; WT, wild-type.

including $CD4^+$ T cell infiltration and IFNγ and TNFα levels. Altogether, these results demonstrate that MLCK activity plays a crucial role in the maintenance of the increased immune response related with barrier dysfunction.

Recent data from the literature support the opinion that *Nod2* mediates an immune tolerance towards bacterial products in human and mouse.[2 3] Chronic stimulation of NOD2 results in a decreased production of inflammatory mediators in response to subsequent TLR2/4 stimulation in human macrophages.[2 3] This immune tolerance affects the production of TNFα, a cytokine with a central role in the pathogenesis of Crohn·s disease.[48] NOD2 inhibits the TLR2 pathway by blocking the nuclear translocation of C-Rel.[5] This inhibitory effect is mediated by an upregulation of IRF4 (IFN regulatory factor 4).[49] NOD2 also inhibits the TLR4 pathway. The inhibition of TLR signalling by NOD2 may be pivotal by preventing an excessive gut inflammation driven by the microflora. We report here an over-expression of TLR2/4 mRNA in PP from $Nod2^{-/-}$ mice. In $Nod2^{+/+}$ mice, TLR2/4 stimulation triggers increased antigen permeability and migration of DCs into the FAE. This increased permeability is downregulated by MDP pre-treatment, and is dependent on MLCK activity. It can thus be postulated that the phenotype driven by the ileal microflora in $Nod2^{-/-}$ mice is related with the activation of the TLR pathways.

$Nod2^{-/-}$ mice are characterised by an excess of bacterial translocation. This effect can be demonstrated in vivo and ex vivo. It seems to be mainly related to PP areas, bacterial translocation across PP-free ileal mucosa being comparable between $Nod2^{+/+}$ and $Nod2^{-/-}$ mice. Finally, PP abnormalities are also observed in the mutated mice $Nod2^{mut/mut}$ which carry the mutation homologous with the most comprehensive mutation in humans. This finding suggests it would be useful to further explore the functions of PPs in human diseases, namely Crohn·s disease and GVHD.

Funding This work was supported by the Institut National de la Santé et de la Recherche Médicale, la Mairie de Paris, BREMICI, Association François Aupetit, Fondation pour la Recherche Médicale and the National Institute of Health.

Competing interests None.

Ethics approval The mice were housed in accordance with the institutional animal healthcare guidelines. The experiments were approved by the institutional committee for animal use.

Provenance and peer review Not commissioned; externally peer reviewed.

REFERENCES

1. **Inohara N,** Nunez G. NODs: intracellular proteins involved in inflammation and apoptosis. *Nat Rev Immunol* 2003;**3**:371–82.
2. **Kullberg BJ,** Ferwerda G, de Jong DJ, *et al*. Crohn's disease patients homozygous for the 3020insC NOD2 mutation have a defective NOD2/TLR4 cross-tolerance to intestinal stimuli. *Immunology* 2008;**123**:600–5.

3. **Hedl M,** Li J, Cho JH, *et al*. Chronic stimulation of Nod2 mediates tolerance to bacterial products. *PNAS* 2007;**104**:19440—5.
4. **Netea MG,** Ferwerda G, de Jong DJ, *et al*. Nucleotide-binding oligomerization domain-2 modulates specific TLR pathways for the induction of cytokine release. *J Immunol* 2005;**174**:6518—23.
5. **Yang Z,** Fuss IJ, Watanabe T, *et al*. NOD2 transgenic mice exhibit enhanced MDP-mediated down-regulation of TLR2 responses and resistance to colitis induction. *Gastroenterology* 2007;**133**:1510—21.
6. **Hugot JP,** Chamaillard M, Zouali H, *et al*. Association of NOD2 leucine—rich repeat variants with susceptibility to Crohn's disease. *Nature* 2001;**411**:599—603.
7. **Ogura Y,** Bonen DK, Inohara N, *et al*. A frameshift mutation in NOD2 associated with susceptibility to Crohn's disease. *Nature* 2001;**411**:603—6.
8. **Sartor RB.** Current concepts of the etiology and pathogenesis of ulcerative colitis and Crohn's disease. *Gastroenterol Clin North Am* 1995;**24**:475—507.
9. **Elmaagacli AH,** Koldehoff M, Hindahl H, *et al*. Mutations in innate immune system NOD2/CARD 15 and TLR-4 (Thr399Ile) genes influence the risk for severe acute graft-versus-host disease in patients who underwent an allogeneic transplantation. *Transplantation* 2006;**81**:247—54.
10. **Holler E,** Rogler G, Herfarth H, *et al*. Both donor and recipient NOD2/CARD15 mutations associate with transplant-related mortality and GvHD following allogeneic stem cell transplantation. *Blood* 2004;**104**:889—94.
11. **Finch PW,** Rubin JS. Keratinocyte growth factor/fibroblast growth factor 7, a homeostatic factor with therapeutic potential for epithelial protection and repair. *Adv Cancer Res* 2004;**91**:69—136.
12. **Gerbitz A,** Schultz M, Wilke A, *et al*. Probiotic effects on experimental graft-versus-host disease: let them eat yogurt. *Blood* 2004;**103**:4365—7.
13. **Holler E,** Rogler G, Brenmoehl J, *et al*. Prognostic significance of NOD2/CARD15 variants in HLA-identical sibling hematopoietic stem cell transplantation: effect on long-term outcome is confirmed in 2 independent cohorts and may be modulated by the type of gastrointestinal decontamination. *Blood* 2006;**107**:4189—93.
14. **Fujimura Y,** Kamoi R, Iida M. Pathogenesis of aphthoid ulcers in Crohn's disease: correlative findings by magnifying colonoscopy, electron microscopy, and immunohistochemistry. *Gut* 1996;**38**:724—32.
15. **Murai M,** Yoneyama H, Ezaki T, *et al*. Peyer's patch is the essential site in initiating murine acute and lethal graft-versus-host reaction. *Nat Immunol* 2003;**4**:154—60.
16. **Barreau F,** Meinzer U, Chareyre F, *et al*. CARD15/NOD2 is required for Peyer's patches homeostasis in mice. *PLoS One* 2007;**2**:e523.
17. **Kuhn R,** Lohler J, Rennick D, *et al*. Interleukin-10-deficient mice develop chronic enterocolitis. *Cell* 1993;**75**:263—74.
18. **Devlin SM,** Yang H, Ippoliti A, *et al*. NOD2 variants and antibody response to microbial antigens in Crohn's disease patients and their unaffected relatives. *Gastroenterology* 2007;**132**:576—86.
19. **Katz KD,** Hollander D, Vadheim CM, *et al*. Intestinal permeability in patients with Crohn's disease and their healthy relatives. *Gastroenterology* 1989;**97**:927—31.
20. **Maeda S,** Hsu LC, Liu H, *et al*. Nod2 mutation in Crohn's disease potentiates NF-kappaB activity and IL-1beta processing. *Science* 2005;**307**:734—8.
21. **Ghiasi H,** Cai S, Perng GC, *et al*. Both CD4+ and CD8+ T cells are involved in protection against HSV-1 induced corneal scarring. *Br J Ophthalmol* 2000;**84**:408—12.
22. **Gulig PA,** Doyle TJ, Clare-Salzler MJ, *et al*. Systemic infection of mice by wild-type but not Spv-Salmonella typhimurium is enhanced by neutralization of gamma interferon and tumor necrosis factor alpha. *Infect Immun* 1997;**65**:5191—7.
23. **Ferrier L,** Mazelin L, Cenac N, *et al*. Stress-induced disruption of colonic epithelial barrier: role of interferon-gamma and myosin light chain kinase in mice. *Gastroenterology* 2003;**125**:795—804.
24. **Wang F,** Schwarz BT, Graham WV, *et al*. IFN-gamma-induced TNFR2 expression is required for TNF-dependent intestinal epithelial barrier dysfunction. *Gastroenterology* 2006;**131**:1153—63.
25. **Blair SA,** Kane SV, Clayburgh DR, *et al*. Epithelial myosin light chain kinase expression and activity are upregulated in inflammatory bowel disease. *Lab Invest* 2006;**86**:191—201.
26. **Chabot S,** Wagner JS, Farrant S, *et al*. TLRs regulate the gatekeeping functions of the intestinal follicle-associated epithelium. *J Immunol* 2006;**176**:4275—83.
27. **Netea MG,** Ferwerda G, de Jong DJ, *et al*. NOD2 3020insC mutation and the pathogenesis of Crohn's disease: impaired IL-1beta production points to a loss-of-function phenotype. *Neth J Med* 2005;**63**:305—8.
28. **Neutra MR,** Mantis NJ, Kraehenbuhl JP. Collaboration of epithelial cells with organized mucosal lymphoid tissues. *Nat Immunol* 2001;**2**:1004—9.
29. **Cebra JJ,** Sterzl J, *et al*. The role of mucosal microbiota in the development and maintenance of the mucosal immune system. In: Ogara PL**,** Lamm ME, Bienenstock C, *et al*, eds. *Mucosal immunology* San Diego: Academic Press, 1999:267—80.
30. **Iiyama R,** Kanai T, Uraushihara K, *et al*. Normal development of the gut-associated lymphoid tissue except Peyer's patch in MyD88-deficient mice. *Scand J Immunol* 2003;**58**:620—7.
31. **Niess JH,** Leithauser F, Adler G, *et al*. Commensal gut flora drives the expansion of proinflammatory CD4 T cells in the colonic lamina propria under normal and inflammatory conditions. *J Immunol* 2008;**180**:559—68.
32. **Yaguchi Y,** Fukatsu K, Moriya T, *et al*. Influences of long-term antibiotic administration on Peyer's patch lymphocytes and mucosal immunoglobulin A levels in a mouse model. *JPEN J Parenter Enteral Nutr* 2006;**30**:395—8; discussion: 99.
33. **Butler M,** Chaudhary R, van Heel DA, Playford RJ, *et al*. NOD2 activity modulates the phenotype of LPS-stimulated dendritic cells to promote the development of T-helper type 2-like lymphocytes—Possible implications for NOD2-associated Crohn's disease. *J Crohn and Colitis* 2007;**1**:106—15.
34. **Wofsy D,** Seaman WE. Reversal of advanced murine lupus in NZB/NZW F1 mice by treatment with monoclonal antibody to L3T4. *J Immunol* 1987;**138**:3247—53.
35. **Christadoss P,** Dauphinee MJ. Immunotherapy for myasthenia gravis: a murine model. *J Immunol* 1986;**136**:2437—40.
36. **Sadlack B,** Merz H, Schorle H, *et al*. Ulcerative colitis-like disease in mice with a disrupted interleukin-2 gene. *Cell* 1993;**75**:253—61.
37. **Powrie F,** Leach MW, Mauze S, *et al*. Phenotypically distinct subsets of CD4+ T cells induce or protect from chronic intestinal inflammation in C. B-17 scid mice. *Int Immunol* 1993;**5**:1461—71.
38. **Stronkhorst A,** Radema S, Yong SL, *et al*. CD4 antibody treatment in patients with active Crohn's disease: a phase 1 dose finding study. *Gut* 1997;**40**:320—7.
39. **Mullin JM,** Snock KV. Effect of tumor necrosis factor on epithelial tight junctions and transepithelial permeability. *Cancer Res* 1990;**50**:2172—6.
40. **Taylor CT,** Dzus AL, Colgan SP. Autocrine regulation of epithelial permeability by hypoxia: role for polarized release of tumor necrosis factor alpha. *Gastroenterology* 1998;**114**:657—68.
41. **Musch MW,** Clarke LL, Mamah D, *et al*. T cell activation causes diarrhea by increasing intestinal permeability and inhibiting epithelial Na+/K+-ATPase. *J Clin Invest* 2002;**110**:1739—47.
42. **Brown GR,** Lindberg G, Meddings J, *et al*. Tumor necrosis factor inhibitor ameliorates murine intestinal graft-versus-host disease. *Gastroenterology* 1999;**116**:593—601.
43. **Suenaert P,** Bulteel V, Lemmens L, *et al*. Anti-tumor necrosis factor treatment restores the gut barrier in Crohn's disease. *Am J Gastroenterol* 2002;**97**:2000—4.
44. **Moriez R,** Salvador-Cartier C, Theodorou V, *et al*. Myosin light chain kinase is involved in lipopolysaccharide-induced disruption of colonic epithelial barrier and bacterial translocation in rats. *Am J Pathol* 2005;**167**:1071—9.
45. **Zolotarevsky Y,** Hecht G, Koutsouris A, *et al*. A membrane-permeant peptide that inhibits MLC kinase restores barrier function in in vitro models of intestinal disease. *Gastroenterology* 2002;**123**:163—72.
46. **Clayburgh DR,** Barrett TA, Tang Y, *et al*. Epithelial myosin light chain kinase-dependent barrier dysfunction mediates T cell activation-induced diarrhea in vivo. *J Clin Invest* 2005;**115**:2702—15.
47. **Scott KG,** Meddings JB, Kirk DR, *et al*. Intestinal infection with *Giardia* spp. reduces epithelial barrier function in a myosin light chain kinase-dependent fashion. *Gastroenterology* 2002;**123**:1179—90.
48. **Targan SR,** Hanauer SB, van Deventer SJ, *et al*. A short-term study of chimeric monoclonal antibody cA2 to tumor necrosis factor alpha for Crohn's disease. *N Engl J Med* 1997;**337**:1029—35.
49. **Watanabe T,** Asano N, Murray PJ, *et al*. Muramyl dipeptide activation of nucleotide-binding oligomerization domain 2 protects mice from experimental colitis. *J Clin Invest* 2008;**118**:545—9.